Material Properties are Related to Stress Fracture Callus and Porosity of Cortical Bone Tissue at Affected and Unaffected Sites

Rachel C. Entwistle, Sara C. Sammons, Robert F. Bigley, Scott J. Hazelwood, David P. Fyhrie, Jeffery C. Gibeling, Susan M. Stover

ABSTRACT: Stress fractures are overuse injuries of bone that affect elite athletes and military recru ts. One response of cortical bon stress fracture is to lay down periosteal callus. The objectives of this study were to determine if material properties are different among b with different stages of stress fracture callu , at both a callus site and at a distal site. Cortical specimens were mechanically teste determine their stress–strain response. Material property differences were examined using nonparametric and regression analyses. At callus site, material properties were low during the earliest stages of callus, higher with increasing callus maturity, but dropped at the stage of callus At the distal site, the material properties were low during early stages of callus and approached, or returned to, those of b without callus during the late stages of callus. The effects of stress fracture and bone callus are not limited to the focal site of stress fracture

Bones modify structure in response t increase magnitudes of repetitive loading[1–4] Cyclic loads, near the upper limit of physiologic loads lea to micr damage accumulation.[4,5] The presence of microdamage stimulates bone remodeling that remove micro damage. [1,3,5] Healthy bone maintenance involves **a** a balance between damaged tissue remova and new tissue deposition.

Stress fractures occur when tissue damag over whelms the repair response Stress fractures are overus injuries of bone that occur in elite athletes and militar recruits. [6–9] Most stress fractures hea with individual returning to full athletic or job performance. Howeve some recur and others progress to complete fracture. clinical index of suspicion is important when patients ar at risk for complete bone fracture Understanding th progression of events would also be useful for design rehabilitation programs. However the events that occu in stress fracture disease are unknown, largely becaus bone specimens are difficult to obtain

Stress fractures are common in equine athletes[10,11] In some racehorses stress fractures progress to complet fracture. 10, 12 Complete fractures are associated with preexisting stress fractures for scapular, humera , thir metacarpal, pelvic, and tibia bones[13–15] Racehorses that sustain a complete fracture may be euthanized, an often have bilateral stress fracture disease Thus, a opportunity exists to investigate the event i th development and progression of stres fracture b examining intact bones of horses with and without stres fracture.

The earliest events in stres fractur diseas ar difficult to detect in clinical patients. Radiographic sign include incomplete fracture and callus formation, whic
are not evident unti late in th diseas proces However, scintigraphy and magnetic resonance imagin (MRI) findings indicate that bone inflammatio and edema are present before callu is observed[11,16] Changes in the parent cortica bone tissue associate with initiation, progression and resolution of stres fractures and their relationship to clinically detectabl features are unknown In addition the extent **of** of fun tional compromise of parent bone tissue during stres fracture development and resolution is unknown

The focus of this study was to determine the function consequences of stress fracture disease by investigatin equine humeri with visible evidence of bone patholog at postmortem examination We hypothesized that (1 material properties of cortical tissue affected with stres fracture are reduced in early stages of callus develo ment because cortical porosity i high (2 materi properties would return to norma with progressiv maturation, and (3) dista bone material would not b affected by callus maturity

MATERIALS AND METHODS

Specimen Categorization and Preparation

Equine humeri were chosen because bone were availabl through the California Horse Racing Board Postmortem Program, and because equine humeri are predisposed to stre fracture in the cauda cortex of the neck[12] Eighteen humeri, obtained postmortem from 18 Thoroughbred racehorse (6 female, 7 gelding, 5 male 2–4 years) were studied. Hume were categorized as affected or control using the presence absence, respectively, of periosteal callus at the proximocaud aspect of the humera neck

Periosteal callus was further categorized into three pr gressive stages using cortica surface elevation color an texture criteria. Stage **1**1 callu wa characterize by n or minimal (<0.5 mm) periosteal surface elevation and red brown discoloration compatible with hemorrhage or hyperemi typical of the parent cortical surface (n = 3) (Fig. 1) Stage 2 wa characterized by periosteal new bone from 0.5-to 2-mm thic discoloration, and soft, rough surface texture typical of woven bone (n = 3). Stage 3 was characterized by periosteal new bone >2-mm thick, discoloration, and a firm surface typical of consolidating bone tissue (n = 2). Control bones (n = 10) were categorized as Stage 0 or Stage 4 callus n separate analyses, the two classifications being based on theoretical scenarios. As Stage 0 callus, control bones were theorized to be nai¨ve bones that were unadapted to race training and racing, and consequently developed stress fracture disease on the way to full adaptation. In this circumstance, the material properties of control bones (Stage 0) could be lower than those of Stages 1, 2, or 3 callus bones. Alternately asStage 4 callus, control bones were theorized to be fully adapted to raining nd acing, and consequently incurred disease. In this circumstance, the properties of control bones (Stage 4) would be higher than those of Stage 1, 2, and 3 bones. This categorization allowed for investigation of linear relationships with progression of callus maturity relative to a na¨ıve or fully adapted state.

Two bone tissue specimens were harvested from each humerus for mechanical testing. Because bone tissue availability was limited, a cortical beam was harvested rom he proximocaudal site predisposed to stress fracture Fig. 2). A cortical core was harvested from a nonaffected site of he diaphyseal cortex, about 35 mm distal to the proximocaudal site (Fig. 2). Cortical beams (3 x 3 x 36 mm) were machined from parent cortical bone using a CNC mill to minimize inclusion of periosteal callus. Rightcylindrical cores were cut with heir long axis parallel to the longitudinal axis of the bone ortex. Cores (6-mm diam., 15-mm long) were drilled using a hollow, diamond-tipped drill bit at 720 rpm while rrigated with cool saline. All specimens were stored in calcium-buffered saline-soaked gauze at -20°C until testing.[17]

Mechanical Testing

Specimens were thawed to room temperature (25°C) on the day of testing. Beams were subjected to hree-point bending to failure with the periosteal surface n compression support span: 28 mm) at an apparent surface strain rate of 0.01 $^{-1}$ (percent overhang at the ends was determined using ASTM D 6272-02 and general setup using ANSI/ASAE S459 DEC01). Cores were compressed between parallel steel platens n a single load to failure at an apparent strain rate of 0.01 s $^{-1}$ [ASTM E 9-89a (Reapproved 2000)]. Mechanical tests used a servohydraulic materials testing system Model 809; MTS Systems Corp., Minneapolis, MN) running Testware SX software. Load (MTS Systems Corp. load cell; 2000 N for
beams; 15,000 N for cores) and actuator displacement data were collected at a rate of 20 Hz during all tests, nd were converted to stress and strain using specimen geometries and original lengths.

Material properties were derived from stress versus strain curves using a custom Matlab® program (MathWorks, Inc., Natick, MA).[18] The yield point was determined using a 0.02% strain offset method.[19] The ultimate point was defined at maximum stress. An initial toe region was evident n he stress versus strain curves for the cortical cores. Consequently, strains and strain energy densities SEDs) were determined between the end of the toe region and respective points. The end of the toe region was identified using a 0.015% reverse offset method. Apparent elastic modulus was determined using linear regression for data between 15 and 45% (beams) and 25 and 70% (cores) of the ultimate strength. These were the greatest ranges (in the linear region) that applied to all beams or cores. SEDs at yield and ultimate were calculated using a middle Riemann sum technique to each respective point.[20] Post-yield strains and SEDs were also calculated between the yield and ultimate points.

Statistical Analyses

The effect of callus stage on material properties was assessed using nonparametric statistical tests (SAS Institute Inc., Cary, NC). Material property differences among callus stages were examined first using a Kruskal-Wallis test $p < 0.05$). Pairwise differences were examined using a one-sided post-hoc Wilcoxon test ($p < 0.10$) and a Bonferroni correction for experiment-wise error ($p < 0.017$ for each comparison), because the values for diseased bones were expected to be lower than values for control bones. A values of $p < 0.10$ was chosen to detect interesting and useful differences because of the small sample size. Results are also reported for $p < 0.017$.

The existence and nature of any potential linear relationship between bone material properties and callus maturity were explored using univariate linear regression analyses (SAS Institute Inc.). We assumed that allus maturity would influence bone material properties. We chose to treat callus maturity in two ways: (1) assuming that na¨ıve, unadapted bone material developed disease and increasing callus maturity results in successful adaptation and enhanced material properties (Stages 0, 1,1, 2, and 3), and (2) assuming that fully adapted bone material with optimum material properties developed disease that compromised material properties control bones (Stage 0) were reclassified as Stage 4 (Stages 1,1, 2,2, 3, and 4). Statistical significance was defined as $p < 0.05$

and statistical trends were defined as $0.05 < p < 0.10$.

Morphological Analysis

Porosity was measured to determine f morphologic changes were related to material property differences among allus stages. Transverse sections (3-mm thick) were harvested from all specimens after mechanical testing. Specimens were fixed in ethanol (4 days at 65%, 4 days at 85%), dehydrated, cleared, infiltrated, and embedded in plastic Technovit 7200, Heraeus Kulzer GmbH, Germany). Embedded sections were mounted (Technovit 4000 and 7210, Heraeus Kulzer GmbH, Germany) on plastic slides and ground to an average thickness of 90 μm (EXAKT 400 CS grinder, EXAKT Apparatebau GmbH & Co., Germany).

High-detail radiographs (Faxitron 805 X-ray cabinet, Field Emission Corp., McMinnville, OR) of each slide were obtained using an emulsion film technique (AGHD High-Definition glass plates with type 2 HDEmulsion, HTA Enterprises, San Jose, CA) (40 min, 14 kVp, 3 mA). Radiographs were digitized using transmitted ight microscopy VANOX-T, Olympus America Inc., Center Valley, PA) and a PAXcam3 in conjunction with PAX-it! software (MIS Inc., Villa Park, IL). A custom Matlab [1] program was used to import digitized mages and produce binary images from which a porosity measurement was obtained for beams (Fig. 3) and cores (Fig. 4). The threshold for each binary image was subjectively chosen from a gray-level (bimodal) histogram. The initial rising edge of the right-most peak (representing the white peak) was chosen to separate bone from void space. From the thresholded image, porosity (%) was calculated by dividing the number of pixels below bone threshold (black) by the total number of pixels and multiplied by 100. The central portion of each section was used to measure porosity (about 2.3 x 2.3 mm square for cortical beams, 4.4 mm diameter circle (or largest possible area if the section was not circular due to fragment shape after the mechanical tests) for cortical cores).

A Kruskal-Wallis test was used to examine the effects of callus stage with porosity ($p < 0.05$) (SAS Institute Inc., Cary, NC). A Wilcoxon post-hoc analysis was used to examine differences among callus stages (Stage 0,1,2,3). For the purpose of detecting interesting and potentially useful differences in the post-hoc analysis, and due to small samples sizes among callus stages, significance was set at $p < 0.10$ (Bonferroni $p < 0.017$). Relationships between the measured material properties and porosity were examined using univariate linear regression (SAS Institute Inc.). We assumed that porosity would influence bone material properties. Significance was defined as $p < 0.05$, and trends were defined as $0.05 < p < 0.10$.

RESULTS

Cortical Beam Material from the Proximocaudal Site Predisposed to Stress Fracture

Several material properties were different among callus stages (Table 1) Stage 3 callus specimens had lower modulus, yield and ultimate strengths, and yield, ultimate, and post-yield SEDs than all other allus stage specimens (including controls) ($p < 0.075$ for all comparisons). Stage 3 callus specimens also had lower yield strain than Stage 0 and Stage callus specimens ($p = 0.075$ for each). Stage 2 callus specimens had higher ultimate and post-yield strains, ultimate strength and SED, and post-yield SED than Stage 1 callus specimens ($p < 0.10$ for all comparisons). Stage 0 callus specimens had higher ultimate SED than Stage pecimens ($p = 0.075$). Using the Bonferroni correction, no significant differences were evident.

Callus maturity was negatively associated with number of material properties for the proximocaudal site when controls were considered as Stage 0 (Table 2). Modulus, yield and ultimate strength, and ultimate and post-yield SEDs all decreased with callus stage ($p <= 0.032$, $R^2 => 0.26$ for all models). There was also a negative trend with yield train p 1/4 0.082, $R^2 <= 0.18$).

At the stress fracture site, porosity was greatest in Stage 3 beams ($p <= 0.075$ for all comparisons) (Table 3). Stages 1 and 2 also had greater porosity than ontrol specimens ($p < 0.038$ for all comparisons). Using the Bonferroni correction, no statistically significant differences were evident. Porosity was negatively related to all material properties ($p < 0.034$, $R^2 > 0.25$ for all models) (Table 4).

Cortical Core Material from a Distal Site

Stage 1 specimens had lower modulus, yield and ultimate strength, and higher ultimate and post-yield strains than Stage 0 $p < 0.075$ for all comparisons) (Table 5). Stage 1 also had lower ultimate strength than Stage 2 ($p = 0.007$). Stage 2 specimens had lower ultimate strength, ultimate nd ostyield trains, ultimate and postyield SED than Stage 0 ($p < 0.054$ for all comparisons). Stage 2 also had lower ultimate strain than Stage 1 ($p = 0.038$). Stage 3 specimens had a higher modulus than Stage 11 ($p = 0.075$). Stage 1 specimens had lower yield strength and higher post-yield strains than Stage 2 or 3 ($p < 0.075$ for all comparisons). Stage 3 specimens had higher ultimate strength than Stage 1 or 2 ($p = 0.075$ for each). Stage 2 specimens had lower ultimate and post-yield SEDs than Stage 0 and Stage 1 1 specimens ($p < 0.054$ for all comparisons). Multiple differences were also found

with the Bonferroni correction. Stage 11 had lower yield strength han tage 0 ($p = 0.011$). Stage 1 also had lower ultimate strength than Stage 0 and Stage 2 $p = 0.007$ for each). Stage 2 had lower ultimate strain than Stage $p = 0.007$). Stage 2 also had lower ultimate SED than Stage ($p = 0.007$).

Callus maturity had moderate to trong positive relationships with modulus and yield and ultimate strengths when controls were considered as Stage 4 ($p < 0.033$, $R^2 > 0.25$ for all models) (Table 2).

Porosity was not different among callus stages for the cortical cores ($p > 0.176$ for each comparison) (Table 3). No significant relationships existed with porosity and any measured material properties ($p > 0.263$, $R^2 < 0.08$ for all models) (Table 4).

DISCUSSION

We examined the effects of stress fracture allus maturity on the material properties of parent cortical bone tissue at a site predisposed to stress fracture and at a distal site. We found that the presence of callus, indicative of stress fracture, was related to a number of material properties of bone tissue at both sites, although the nature of the relationships was different. At the site predisposed to stress fracture, advancing tages of callus maturity were associated with a decrease n modulus, yield, and ultimate strengths, and ultimate and post-yield SEDs compared to bones without callus indicative of stress fracture. At the distal site, advancing stages of callus maturity were associated with an increase in modulus, and yield and ultimate strengths thatculminated n values approaching those of bones without callus at the site predisposed to stress fracture. Porosity was observed to increase with advancing stage of callus and decreasing material properties at the affected site, but not at the distal s te.

Cortical bone tissue subjacent to callus at the stress fracture site was mechanically compromised, attempted to recover early with increasing callus maturity, but decompensated with the most mature allus. Decompensation is the inability ofcompromised bone material to function appropriately when continually subjected to load induced stresses and strains. The mechanical behavior of the parent bone tissue subjacent to callus generally progressed toward that of bones without callus with advancing callus maturity through Stages 1 and 2. However, for every measured material property the median value for Stage 3 callus bones was the lowest of all stages The Stage 3 specimens in this study were likely decompensated.

Material properties ofcortical bone tissue at the distal site changed in conjunction with the presence of stress fracture. We hypothesized that material away from the stress fracture site would be unaffected. The opposite finding indicates that the factors inducing stress fracture are not isolated to the focal site of fracture However, the effects were different between the two sites. At the distal site, material properties were low during the early stages of periosteal callus formation but ncreased with callus maturity The material properties of bones with Stage 3 callus approximated those of unaffected bones. These findings indicate that the distal ite is able to adapt successfully to the loading factors that induced stress fracture at the stress fracture site.

A likely mechanism for decompensation at the fracture site is increased porosity n the bone issue. Porosity accounted for 25–65% f the variability inin material properties at the affected site. Material properties at the affected ite ppeared o ncrease with advancing callus, but dropped dramatically at the late stage of callus. Porosity however increased in early stages of callus and continued to do so in the late stages. With less bone material present, the bone s not s strong, and the structure may be ncapable of withstanding normal loads. Porosity differences were not observed among callus stages for the distal site. However, the distal site experienced low material properties in the early stages of callus. Other unmeasured morphological variables could contribute to the observed changes in the properties at the distal site.

The most mechanically compromised bone tissue occurred with the earliest ndication of bone damage and ‘‘pending’’ periosteal callus formation. The only exception was the decompensated Stage 3 allus bone specimens from the stress fracture site. For all other specimens from both sites, median values for modulus and yield and ultimate strengths were lowest for Stage 1 callus. At the stress fracture ite, typical signs of bone disease were limited to regional red-brown discoloration of a smooth parent bone surface. Previously this change was often interpreted as postmortem artifact from blood staining. However, our findings indicate that discoloration is compatible with inflammation of parent cortical bone tissue. Bone discoloration preceded periosteal woven bone production.

Our classification system is consistent with he natural progression of bone healing after trauma. The response of bone to fracture occurs in three phases.[21] The initial inflammatory phase isis dominated by cellular infiltration, edema, and hyperemia (comparable to Stage 1). Subsequently, the reparative phase s characterized by woven bone callus formation that s highly vascular and coarse (comparable to Stage 2). The final remodeling phase is characterized by replacement of woven bone with lamellar bone that is smooth and hard (comparable to Stage 3).

The lack of observed differences between yield strains among bones with callus, and among bones without callus, is consistent with the concept of strain controlled bone failure.[22] Except for Stage 3 callus specimens at the

site of stress fracture, a common median yield strain occurred across a 13% range of median yield strengths for specimens from both sites. This is consistent with the study of Nalla et al.[22] where double-notched cortical beams from normal human humeri were tested in four-point bending. That study indicated that crack formation occurs at the notch tip (strain controlled failure) rather than in the tissue away from the tip (stress controlled failure). Bone's elastic behavior before yield is modulated by mineralization and collagen quality[23,24] No known biological reason that would lead to abnormal mineralization and collagen quality in bones from the young equine athletes exists for the urrent tudy. Because yield strain differences were not seen between specimens with and without stress fracture, there is no reason to suspect abnormal mineralization and collagen quality. The same initial failure mechanism likely occurred in each specimen.

Our results could be affected by two aspects of the study sample. First, only humeri from horses that died because of a catastrophic injury were included. All horses with a humerus that had periosteal callus died because of a complete contralateral humeral fracture (eight horses). Horses without callus died from catastrophic musculoskeletal injuries unrelated to the humerus (nine horses) or from pulmonary hemorrhage (one horse). All complete fractures were associated with a preexisting tress fracture because affected horses usually have bilateral stress fracture disease. [14,25] We examined the contralateral humeri to investigate he bone material changes that preceded complete fracture. An advantage is that these bones will not have additional damage associated with catastrophic fracture. Successful humeral adaptation is characterized by blunting of the curvature of the humeral neck indicative of periosteal bone modeling and increased cortical area. All horses affected with humeral stress fracture and periosteal bone production ikely experience similar early events or perturbations to parent cortical bone tissue. However, subsequent material property changes may differ between those horses that sustain catastrophic fracture and those that do not. Second, sample size was limited by the availability of equine humeri with stress fractures and stress remodeling at the proximocaudal aspect of the humeral neck. [14] Although there isis reasonable confidence that observed differences are real, the power of our conclusions of no difference among groups is low. However, median values among groups with no significant differences were similar in magnitude.

For the pairwise comparisons between stages, differences were determined based on two cutoff values for significance. To avoid experiment-wise error, a Bonferroni correction was used. Although decreasing the likelihood of a type II error, this correction increases the probability of obtaining type I errors. [26] We were most interested n detecting otentially mportant differences among callus groups rather than eliminating the probability of accepting the null hypothesis no differences exist between specific groups) when it s not true. Consequently, we felt it equally important to mention differences between callus groups at the $p < 0.10$ level rather than at the $p < 0.017$ level only. Although some of our significant results (at $p < 0.10$) may be attributed to ype I error approximately 1 in 10), many of the other differences are likely to be true. The probable cause of our inability to achieve significant differences under the Bonferroni correction was the small sample sizes among callus groups.

The confounding effects of age and sex on the relationship between callus maturity and material properties would be useful to examine in future studies. Unfortunately our sample size was too small to allow for simultaneous consideration of multiple factors.

Our results likely apply to other animals and humans. Regardless of species, stress fractures occur with similar clinical features in individuals undergoing repetitive activities at elite evels or heir espective sport or occupation. Bone edema is first discernible on MRI. Focal regions of increased radiopharmaceutical uptake are visible on scintigraphic images atcharacteristic locations within typical bones related o he specific activity or occupation of the ndividual. Subsequently, periosteal and endosteal bone callus are visible radiographically; in many individuals a radiolucent line recognized as an incomplete fracture isis visualized. Most individuals recover from disease with a period of reduced activity Differences among species are largely related to different activities that induce the repetitive, overuse syndrome, and consequently, the specific bones and regions within bones typically affected with stress fracture.

In summary, the presence of periosteal bone callus indicative of stress fracture reflected degradation f material properties of underlying cortical bone tissue. Cortical tissue at a site distal to the stress fracture also underwent material property changes; however, these changes reflected an adaptive response that resulted in improvement in bone tissue quality. The humeral cortical bone tissue of equine athletes hat died consequent to humeral stress fracture of the contralateral limb appeared to successfully respond to the mechanical signal at the distal tissue site, but succumbed to injury at the site ofcallus accumulation. Bones are weak from the onset of stress fracture and through the stages of healing. From this study bones appear to be most weak when it is difficult to detect stress fracture radiographically (prior to callus formation). Therefore, an individual's activity level should be modified at the earliest ndication of disease. Exuberant periosteal callus is apparently indicative of markedly reduced material properties of parent cortical bone material.

ACKNOWLEDGMENTS

This project was supported by the Center for Equine Health, with funds provided by the State of California parimutuel fund and contributions by private donors. The authors would like to also acknowledge the California Horse Racing Board Postmortem Program and the California Animal Health and Food Safety Laboratory System Veterinary pathologists.

REFERENCES

1. Hsieh YF, Silva MJ. 2002. In vivo fatigue loading of the rat ulna induces both bone formation and resorption and eads to time-related changes n bone mechanical properties and density. J Orthop Res 20:764–771.
2. Wallace JM, Rajachar RM, Allen MR, et al. 2007. Exercise-induced changes in the cortical bone of growing mice are bone-and gender-specific. Bone 40:1120–1127.
3. Lieberman DE, Pearson OM, Polk JD, et al. 2003. Optimization of bone growth andremodeling in response to oading in tapered mammalian limbs. J Exp Biol 206:3125–3138.
4. Schaffler MB, Radin EL, Burr DB. 1989. Mechanical and morphological effects of strain rate on fatigue of compact bone. Bone 10:207–214.
5. Burr DB, Martin RB, Schaffler MB, et al. 1985. Bone remodeling in response to in vivo fatigue microdamage. J Biomech 18:189–200.
6. Hetsroni I, Finestone A, Milgrom C, et al. 2008. The role of foot pronation in the development of femoral and tibial tress fractures: a prospective biomechanical study. Clin J Sport Med 18:18–23.
7. Valimaki VV, Alfthan H, Lehmuskallio E, et al. 2005. Risk factors for clinical stress fractures in male military recruits: a prospective cohort study. Bone 37:267–273.
8. Hame SL, LaFemina JM, McAllister DR, et al. 2004. Fractures in the collegiate athlete. Am J Sports Med 32: 446–451.
9. Iwamoto J, Takeda T. 2003. Stress fractures n athletes: review of 196 cases. J Orthop Sci 8:273–278.
10. Verheyen KL, Wood JL. 2004. Descriptive epidemiology of fractures occurring in British Thoroughbred racehorses in training. Equine Vet J 36:167–173.
11. Kraus BM, Ross MW, Boswell RP. 2005. Stress remodeling and stress fracture of the humerus n four standardbred racehorses. Vet Radiol Ultrasound 46:524–528.
12. Carrier TK, Estberg L, Stover SM, et al. 1998. Association between long periods without high-speed workouts and risk of complete humeral or pelvic fracture in thoroughbred racehorses: 54 cases (1991–1994). J Am Vet Med Assoc. 212:1582– 1587.
13. Riggs CM, Whitehouse GH, Boyde A. 1999. Pathology of the distal condyles of the third metacarpal and third metatarsal bones of the horse. Equine Vet J31:140–148.
14. Stover SM, Johnson BJ, DaftBM, et al. 1992. An association between complete and incomplete stress fractures f he humerus in racehorses. Equine Vet J 24:260–263.
15. Stover SM, Ardans AA, Read DH, et al. 1993. Patterns of stress fractures associated with omplete bone fractures in racehorses. 39th Annual American Association of Equine Practitioners (AAEP)Convention.
16. Fredericson M, Jennings F, Beaulieu C, et al. 2006. Stress fractures in athletes. Top Magn ResonImaging 17:309–325.
17. Gustafson MB, Martin RB, Gibson V et al. 1996. Calcium buffering is required to maintain bone stiffness n saline solution. J Biomech 29:1191–1194.
18. Entwistle RC. 2008. Relationships of stress fracture yndrome, bone microstructural features, and exercise history with material properties of humeri from thoroughbred racehorses. In: Biomedical engineering. Davis, CA: University of California, Davis.
19. Martin RB, Gibson VA, Stover SM, et al. 1997. Residual strength of equine bone is not reduced by ntense atigue loading: implications for stress fracture. J Biomech 30:109– 114.
20. Callahan J, Hoffman K. 1995. Calculus in context: The Five College Calculus Project. New York: W.H. Freeman & Company.

21. Cruess RL, Dumont J. 1975. Fracture healing. Can J Surg 18: 403–413.
22. Nalla RK, Kinney JH, Ritchie RO. 2003. Mechanistic fracture criteria for the failure of human cortical bone. Nat Mater 2:164–168.
23. Burstein AH, Zika JM, Heiple KG, et al. 1975. Contribution of collagen and mineral to the elasticplastic properties of bone. J Bone Joint Surg Am 57:956–961.
24. Zioupos P, Currey JD, Sedman AJ. 1994. An examination of the micromechanics of failure of bone and antler by acoustic emission tests andLaser Scanning Confocal Microscopy Med Eng Phys 16:203–212.
25. O'Sullivan CB, Lumsden JM. 2003. Stress fractures of the tibia and humerus in Thoroughbred racehorses: 99 cases (1992–2000). J Am Vet Med Assoc. 222:491–498.
26. Perneger TV. 1998. What's wrong with Bonferroni adjustments. Br Med J 316:1236.

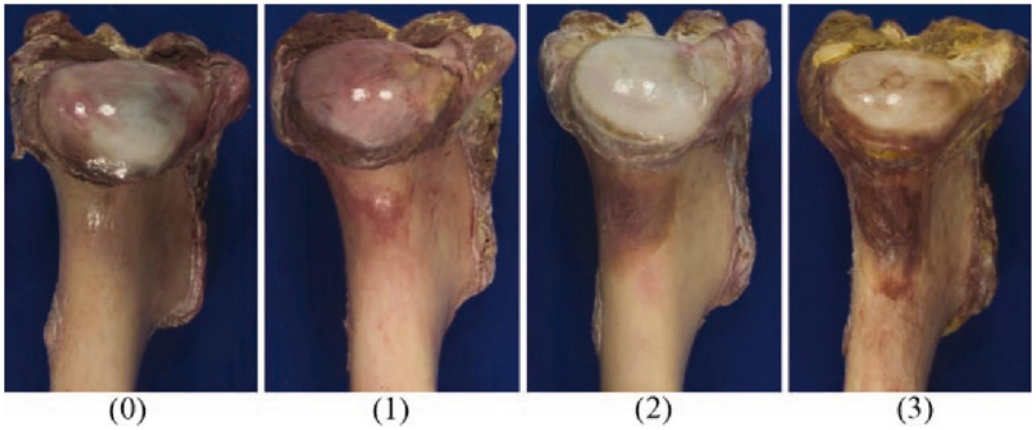

Figure 1. Caudal view of proximal stress fracture site for equine humeri without (Stage 0) and with different Stages (1 –3) of periosteal callus indicative of stress fracture. Increasing cllus maturity is represented by increasing numbers

Figure 2. Lateral radiograph of hemi-sagittal section f he proximal end of an equine humerus illustrating locations (to scale) and orientations of cortical cores dashed ine) relative to cortical beams (solid line).

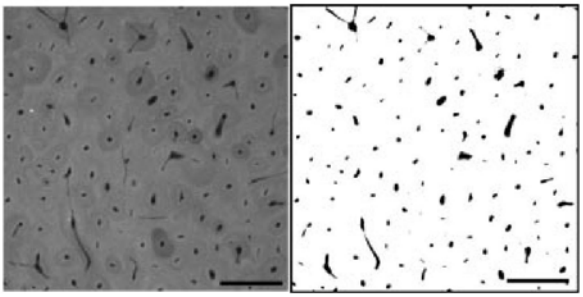

Figure 3. Contact radiograph of a representative ortical beam section (left) and the corresponding thresholded, binary image (right) used for porosity measurement. Bar = 500 µm).

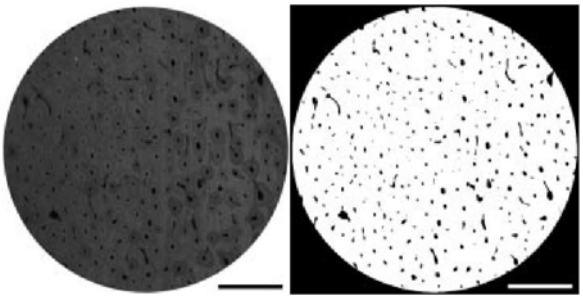

Figure 4. Contactradiograph of a representative ortical core section (left) and the corresponding thresholded, binary image (right) used for porosity measurement. Bar 1/4 1 mm).

Table 1. Material Properties [Median (Range)] at the Proximocaudal Site Predisposed to Stress Fracture for Control and Affected Bones

	Control	Callus Stage		
Material Property	Stage 0	Stage 1	Stage 2	Stage 3
Modulus (GPa)	17.4[a] (15.3–21.0)	15.5[a] (14.0–19.9)	17.3[a] (15.3–19.3)	9.3[b] (6.5–12.2)
Yield strain (µstrain)	8100[a] (7700–9300)	8200[a] (8000–9500)	8200[a,b] (7600–9300)	6600[b] (5600–7600)
Ultimate strain (µstrain)	25,400[a,b] (18,600–28,600)	22,000[a] (21,400–23,400)	24,300[b] (24,200–28,200)	18,200[a,b] (11,900–24,400)
Post-yield strain (µstrain)	17,200[a,b] (10,400–20,700)	13,200[a] (12,500–15,400)	16,700[b] (16,400–18,900)	11,600[a,b] (6300–16,800)
Yield strength (MPa)	145.7[a] (113.8–160.3)	126.8[a] (118.0–149.1)	137.1[a] (137.1–140.4)	59.5[b] (50.0–69.1)
Ultimate strength (MPa)	240.8[a,b] (212.5–287.9)	207.8[a] (202.6–247.4)	253.0[b] (241.4–253.9)	102.5[c] (93.2–111.9)
Yield SED (kJ/m^3)	613[a] (441–685)	585[a] (472–600)	567[a] (537–639)	203[b] (200–206)
Ultimate SED (kJ/m^3)	4178[a] (2799–5161)	3193[b] (2772–3419)	4122[a] (3890–4669)	1161[c] (798–1523)
Post-yield SED (kJ/m^3)	3631[a,b] (2160–4523)	2721[a] (2172–2834)	3585[b] (3322–4030)	958[c] (592–1323)

SED = strain energy density.
[a,b,c]Values that share a superscript within a row are not statistically different ($p < 0.10$).

Table 2. Results from Univariate Regression Analyses for Material Property and Callus Maturity of Cortical Bone Material from the Proximocaudal Site Predisposed to Stress Fracture and a Distal Site

		Stress Fracture Site		Distal Site	
Material Property		Callus Maturity (Control = Stage 0)	Callus Maturity (Control = Stage 4)	Callus Maturity (Control = Stage 0)	Callus Maturity (Control = Stage 4)
Modulus (GPa)	slope	**−2.0**	0.5	−0.1	**0.6**
	intercept	**18.3**	15.1	14.1	**12.3**
	R^2	**0.41**	0.03	0.01	**0.25**
Yield Strain (μstrain)	slope	*−330*	−80	−20	100
	intercept	*8420*	8390	10850	10540
	R^2	*0.16*	0.01	0.00	0.02
Ultimate Strain (μstrain)	slope	−1220	450	−770	−380
	intercept	24020	22240	20320	20830
	R^2	0.10	0.02	0.07	0.02
Post-yield Strain (μstrain)	slope	−850	500	−710	−450
	intercept	16170	13940	9320	10090
	R^2	0.06	0.02	0.07	0.03
Yield Strength (MPa)	slope	**−18.5**	3.6	−1.6	**6.2**
	intercept	**146.0**	119.5	199.1	**178.7**
	R^2	**0.49**	0.02	0.02	**0.30**
Ultimate Strength (MPa)	slope	**−29.4**	5.9	−3.8	**8.1**
	intercept	**249.3**	206.9	246.3	**218.3**
	R^2	**0.43**	0.02	0.11	**0.59**
Yield SED (kJ/m^3)	slope	−63	−12	—9	48
	intercept	563	502	1319	1166
	R^2	0.14	0.01	0.00	0.10
Ultimate SED (kJ/m^3)	slope	**—575**	192	−206	11
	intercept	**4046**	2979	3488	3283
	R^2	**0.30**	0.04	0.14	0.00
Post-yield SED (kJ/m^3)	slope	**—491**	180	—192	—30.6
	intercept	**3436**	2477	2147	2081
	R^2	**0.26**	0.04	0.11	0.00

SED = strain energy density. **Bold** indicates significance ($p < 0.05$); *italics* indicates a statistical trend ($0.05 \leq p < 0.10$).

Table 3. Porosity [Median (Range)] at the Stress Fracture Site and Distal Site for Control and Affected Bones

	Control	Callus Stage		
Porosity (%)	Stage 0	Stage 1	Stage 2	Stage 3
Cortical Beams	4.9[a] (2.9–8.3)	6.9[b] (6.4–10.5)	8.8[b] (6.6–8.9)	18.5[c] (13.0–24.0)
Cortical Cores	4.8[a] (2.5–8.2)	3.7[a] (2.2–4.3)	3.6[a] (3.4–5.5)	13.1[a] (3.4–22.9)

[a,b,c]Values that share a superscript within a row are not statistically different ($p < 0.10$).

Table 5. Material Properties [Median (Range)] at a Site Distal to That Predisposed to Stress Fracture for Control and Affected Bones

	Control	Callus Stage		
Material Property	Stage 0	Stage 1	Stage 2	Stage 3
Modulus (GPa)	14.7[a] (11.5–15.6)	12.8[b] (11.6–13.2)	14.0[a,b] (12.5–14.6)	14.8[a] (13.4–16.1)
Yield Strain (μstrain)	11,000[a] (9600–12,900)	10,800[a] (9200–11,600)	11,100[a] (9600–11,900)	10,900[a] (9700–12,100)
Ultimate Strain (μstrain)	19,400[a] (17,000–25,400)	23,300[b] (21,800–23,800)	16,700[c] (16,700–16,900)	18,300[a,b,c] (14,700–21,900)
Post-yield Strain (μstrain)	8900[a] (5700–13,300)	13,000[b] (10,200–13,200)	5800[c] (4800–7100)	7400[a,c] (5000–9800)
Yield Strength (MPa)	198.4[a] (181.4–226.4)	177.3[b] (176.6–183.3)	204.6[a] (187.1–205.2)	200.5[a] (195.7–205.2)
Ultimate Strength (MPa)	248.3[a] (236.0–267.2)	227.8[b] (221.5–232.1)	232.0[b] (226.2–235.0)	250.2[a] (246.4–254.0)
Yield SED (kJ/m^3)	1291[a] (1091–1684)	1223[a] (950–1261)	1418[a] (1125–1548)	1313[a] (1232–1394)
Ultimate SED (kJ/m^3)	3323[a] (2715–4623)	3948[a] (3448–3963)	2685[b] (2591–2706)	3032[a,b] (2415–3650)
Post-yield SED (kJ/m^3)	2070[a] (1407–2963)	2725[a] (2187–2863)	1287[b] (1043–1560)	1719[a,b] (1183–2256)

SED = strain energy density.
[a,b,c]Values that share a superscript within a row are not statistically different ($p < 0.10$).
Bold superscripts indicate significant differences using the Bonferroni correction ($p < 0.017$).

Table 4. Results from the Univariate Linear Regression Analyses for Cortical Beams between Porosity and Material Properties

Porosity (%)		Modulus (GPa)	Yield Strain (μstrain)	Yield Strength (MPa)	Yield SED (kJ/m^3)	Ultimate Strain (μstrain)	Ultimate Strength (MPa)	Ultimate SED (kJ/m^3)	Postyield Strain (μstrain)	Post-yield SED (kJ/m^3)
Cortical beams	slope	**−0.4**	**−110**	**−4.5**	**−22**	**−570**	**−8.1**	**−186**	**−460**	**−164**
	intercept	**20**	**8990**	**164.5**	**703**	**27910**	**285.3**	**4962**	**18900**	**4259**
	R^2	**0.40**	**0.38**	**0.59**	**0.58**	**0.46**	**0.65**	**0.63**	**0.34**	**0.57**
Cortical cores	slope	−0.1	*90*	0.0	9	190	0.3	34	100	26
	intercept	14.3	*10350*	197.5	1265	18660	241.5	3130	8170	1846
	R^2	0.03	*0.18*	0.00	0.05	0.07	0.01	0.07	0.03	0.04

SED = strain energy density. **Bold** indicates significance ($p < 0.05$); *italics* indicates a statistical trend ($0.05 \leq p < 0.10$).